Adv. Polar Upper Atmos. Res., **14**, 93–102, 2000

Statistical study of Doppler velocity and echo power around 75° magnetic latitude using data obtained with the Syowa East HF radar in 1997

Masaaki Fukumoto[1], Nozomu Nishitani[1], Tadahiko Ogawa[1], Natsuo Sato[2], Hisao Yamagishi[2] and Akira Sessai Yukimatu[2]

[1]*Solar-Terrestrial Environment Laboratory, Nagoya University, Honohara, Toyokawa 442-8507*
[2]*National Institute of Polar Research, Kaga 1-chome, Itabashi-ku, Tokyo 173-8515*

Abstract: We present the statistical relationship between the echo power and Doppler velocity of radar echoes observed with the Syowa East HF radar in Antarctica in 1997. The objective of this analysis was to clarify the mechanisms by which high-latitude (~75° magnetic latitude) *F* region irregularities are generated. Although data points are scattered over a large area, a positive correlation between Doppler velocity and echo power appears to be present. This relationship can be interpreted in terms of gradient-drift instability, which is the most probable cause of the decameter-scale irregularities in the *F* region. The positive correlation deteriorates in the afternoon and midnight sectors, probably as a result of other mechanisms related to particle precipitation (field-aligned current), such as the current-convective instability.

1. Introduction

HF radar can measure echoes backscattered from decameter-scale irregularities in the *E* and *F* regions of the ionosphere (*e.g.*, Greenwald *et al.*, 1985). Three parameters can be derived from the Doppler spectra thus obtained: echo power (signal-to-noise ratio), Doppler velocity (corresponding to line-of-sight plasma velocity), and spectral width. Several studies have been made on the characteristics of VHF and HF radar echoes from the auroral *E* region (*e.g.*, Ogawa and Igarashi, 1982; Hanuise *et al.*, 1991). These studies have revealed various physical properties of the high-latitude *E* region irregularities. In contrast, only a few statistical studies have been performed on high-latitude *F* region echoes. Ruohoniemi and Greenwald (1996, 1997) completed a statistical study on the distribution of the above parameters, but did not investigate the statistical relationship among the parameters.

Two possible mechanisms for the generation of high-latitude *F* region irregularities have been proposed: gradient-drift instability and current-convective instability (*e.g.*, Keskinen and Ossakow, 1983; Tsunoda, 1988). According to linear theories, the growth rate of the gradient-drift instability is proportional to the ambient electric field, while the growth rate of the current-convective instability is proportional to the field-aligned drift velocity of electrons relative to that of ions and is independent of the ambient electric field. For this reason, an analysis of the relationship between echo power and Doppler velocity could provide a clue enabling the mechanisms by which high-latitude *F* region

irregularities are generated to be clarified.

In this paper, we present the statistical relationship between the echo power and Doppler velocity of HF radar echoes from southern high-latitude (~75° magnetic latitude) *F* region irregularities. The statistical relationship between these parameters for data obtained from the Syowa South HF radar was previously presented by our group (Fukumoto *et al.*, 1999). In that study, the data was classified according to the geomagnetic *K* index at Syowa Station. Using this index, we found that the distribution and histograms for each parameter varied slightly, but that the correlations among the parameters did not change very much. We also observed a positive correlation between the echo power and Doppler velocity. However, the dependence of this correlation on the local time or geomagnetic latitude was unknown because the data sampling was too small. Thus, the possible mechanisms responsible for generating *F* region irregularities could not be discussed in detail. In this study, we present a more detailed analysis using a larger amount of data obtained between February 1 and December 31, 1997, using the Syowa East HF radar. The generation of *F* region irregularities is also discussed.

2. Results

Figure 1 shows the field of view of the Syowa East HF radar in geomagnetic coordinates. The data used in this paper was obtained within a range of 1000–1500 km at beam

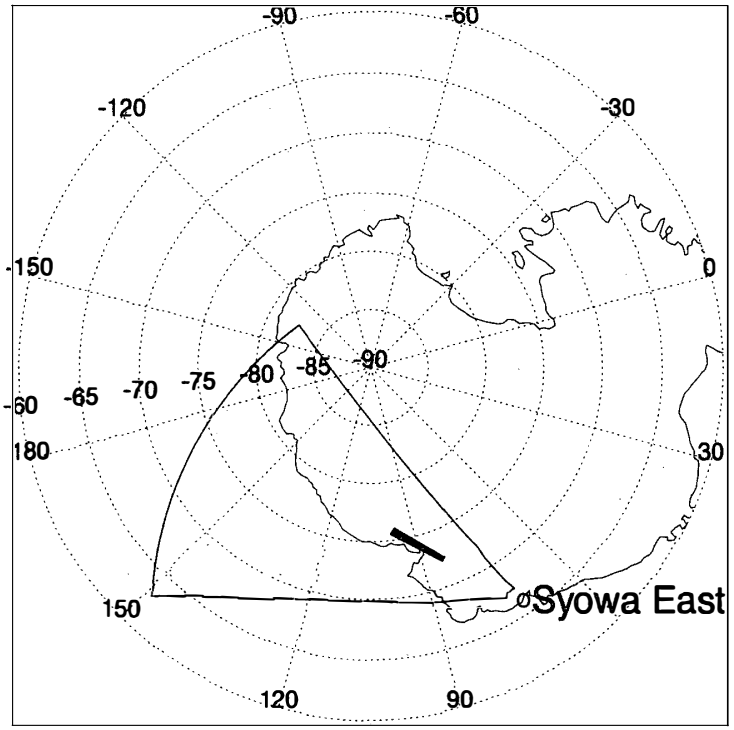

Fig. 1. Field of view of the Syowa Station East HF radar. The magnetic latitude and longitude are given in the Altitude Adjusted Corrected Geomagnetic Coordinate (AACGM) system, which is an updated version of the PACE geomagnetic coordinate system (Baker and Wing, 1989). Data used in this study were obtained at a range of 1000–1500 km on beam 6 (shaded region).

6 (shaded region in Fig. 1) during the period from February 1 to December 31, 1997. This particular range was selected to eliminate the range dependence of the echo power as well as *E* region echoes. *E* region echoes are observed at shorter ranges, while *F* region echoes are observed at farther ranges (*e.g.*, Ogawa *et al.*, 1990). The 1000–1500 km range corresponds to a geomagnetic latitude of 73° to 76°. Magnetic local time (MLT) at the Syowa Station is approximately equal to the universal time (UT). MLT in the region where the echoes are observed is about 1 hour ahead of the Syowa Station MLT.

2.1. Data

In our analysis, echoes with a small Doppler velocity ($|\text{velocity}| \leq 60$ m/s) and a small spectral width (width ≤60 m/s) were regarded as ground scatter echoes and were excluded. To eliminate noise, radio interference and short-lived echoes, spatial and temporal filters were applied to the original data (Fukumoto *et al.*, 1999). The following types of echoes were identified and used in the present study: 1) echoes detected at more than 3 consecutive radar range gates (~90 km) and lasting for more than 2 min (usually for at least two radar scans), and at the same time 2) echoes with Doppler velocities that increase or decrease monotonically over 3 consecutive range gates or that exhibit a small difference (≤33%) between adjacent range gates. In addition, data satisfying at least one of the following criteria was excluded from the study: 1) an echo power of below 0 dB or above 30 dB, 2) a Doppler velocity beyond ±1000 m/s, or 3) a spectral width of above 1000 m/s. Only data satisfying all of the above criteria was used in our analysis.

2.2. Relationship between echo power and Doppler velocity

Figure 2 shows the relationship between the echo power and the Doppler velocity for all data points. The color of each pixel corresponds to the ratio of data points contained in that pixel compared to the total number of data points (53941) included in the analysis. The curve in white shows the median value of the echo power for each Doppler velocity bin. In general, a positive correlation between the echo power and the Doppler velocity can be observed. This finding is consistent with our previous results (Fukumoto *et al.*, 1999). The echo power increases with absolute values of the Doppler velocity up to 500 m/s. Beyond this velocity, the number of data points decreases rapidly, making it difficult to speculate on the relationship between these parameters. The positive correlation between the echo power and the Doppler velocity suggests that the *F* region irregularities are mainly generated by gradient-drift instability. However, the present analysis is insufficient to confirm this suggestion because the data was obtained from all the MLT sectors. The correlation between echo power and Doppler velocity is actually dependent on the MLT, as shown in the next section. Thus, the exact correlation between echo power and Doppler velocity may vary slightly from one MLT region to the next.

2.3. MLT dependence of the correlation between echo power and Doppler velocity

To analyze the data in greater detail, we divided it into 3-hour time intervals. Figure 3 shows the relationship between the echo power and Doppler velocity using the same format as Fig. 2, but for 3-hour intervals. The difference in parameter correlations

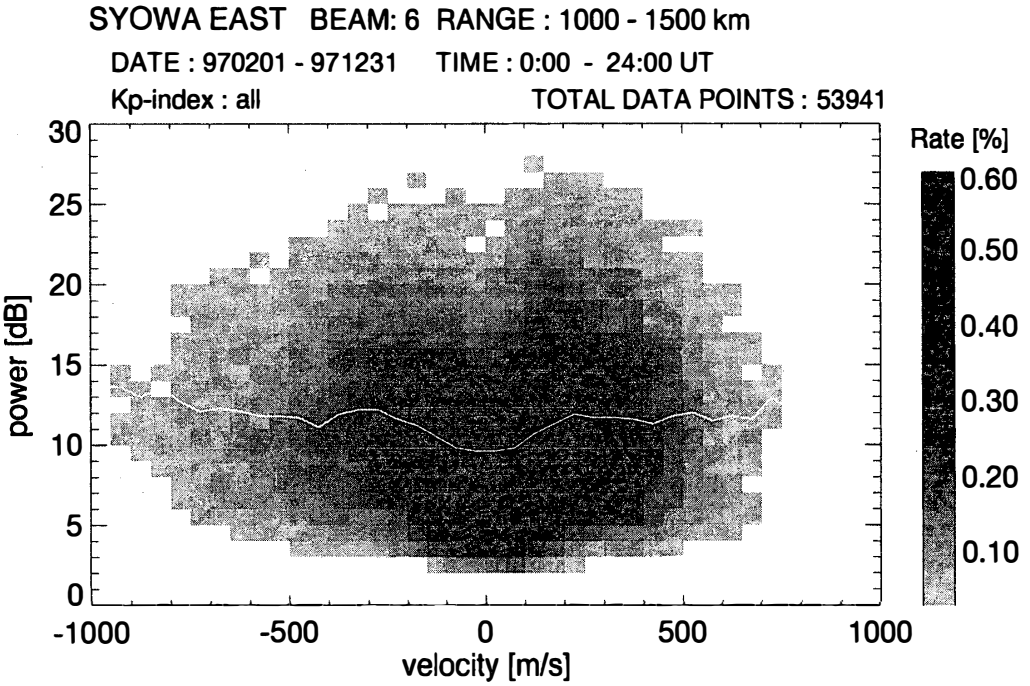

Fig. 2. Relationship between echo power and Doppler velocity for all data points. The color of each pixel corresponds to the ratio of data points contained in that pixel to the total number of data points. The solid curve represents the median value of the echo power in each Doppler velocity bin.

among the eight panels can be clearly seen. Distinct positive correlations can be observed for the time intervals of 0–3 UT, 3–6 UT, 15–18 UT and 18–21 UT. On the other hand, the correlations are poor for the intervals of 6–9 UT, 9–12 UT, 12–15 UT and 21–24 UT. The poor correlations for 6–9 UT, 9–12 UT and 12–15 UT are partly related to the small number of data points for these time intervals. Nevertheless, the differences in these correlations between echo power and Doppler velocity suggest that the primary mechanism for the generation of the *F* region irregularities may also vary. We speculate that for most of the time intervals, the generation of *F* region irregularities is associated with the gradient-drift instability, producing a positive correlation between the echo power and Doppler velocity. On the other hand, for certain time intervals, the generation of the *F* region irregularities may be affected by other mechanisms, such as the current-convective instability, thereby weakening the correlation between echo power and Doppler velocity.

2.4. K_p dependence of the correlation between echo power and Doppler velocity

In the high-latitude ionosphere, particle precipitation from the magnetosphere may play an important role in the generation of *F* region irregularities. To investigate the effect this particle precipitation on the relationship between the echo power and Doppler velocity, the data was sorted according to the K_p index. Figure 4 shows the relationship between the echo power/Doppler velocity correlation and the K_p index for the time interval of 0–3 UT (1–4 MLT), during which period a distinct correlation between echo power and Doppler velocity was present. The upper panel of Fig. 4 shows the data

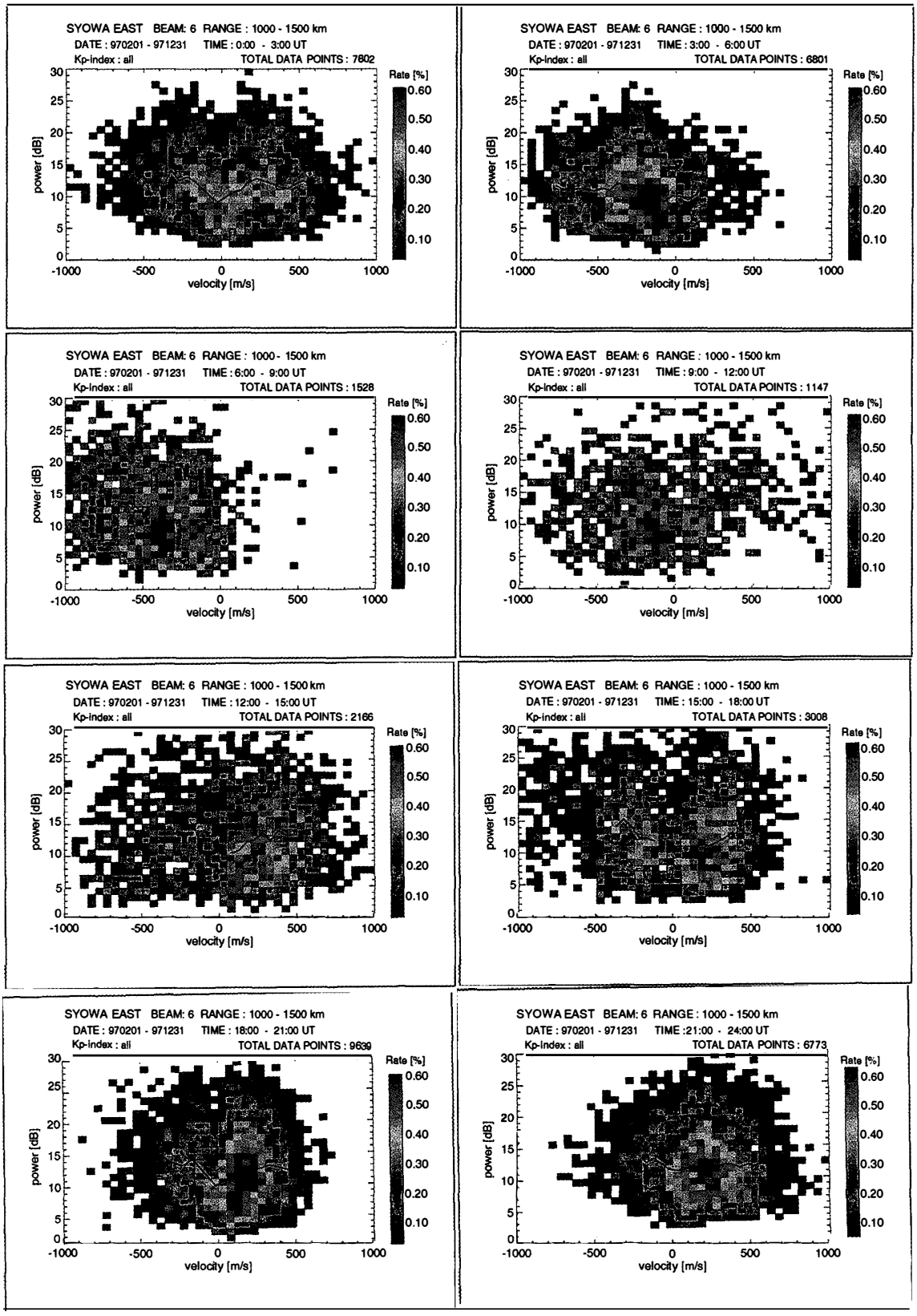

Fig. 3. UT (=MLT-1) dependence of the relationship between echo power and Doppler velocity. The relationship for a three-hour range is plotted in each panel.

obtained under quiet conditions (K_p index ranging from 0 to 1+), while the lower panel shows the data obtained under disturbed conditions (K_p index ranging from 2– to 3+). In the upper panel, a distinct positive correlation is present. In contrast, a poor correlation exists in the lower panel. We speculate that the difference between two panels stems from the effect of particle precipitation on the generation of *F* region irregularities. Under quiet conditions, the *F* region irregularities in this local time sector are mainly generated by gradient-drift instability. Under disturbed conditions, however, the generation of the

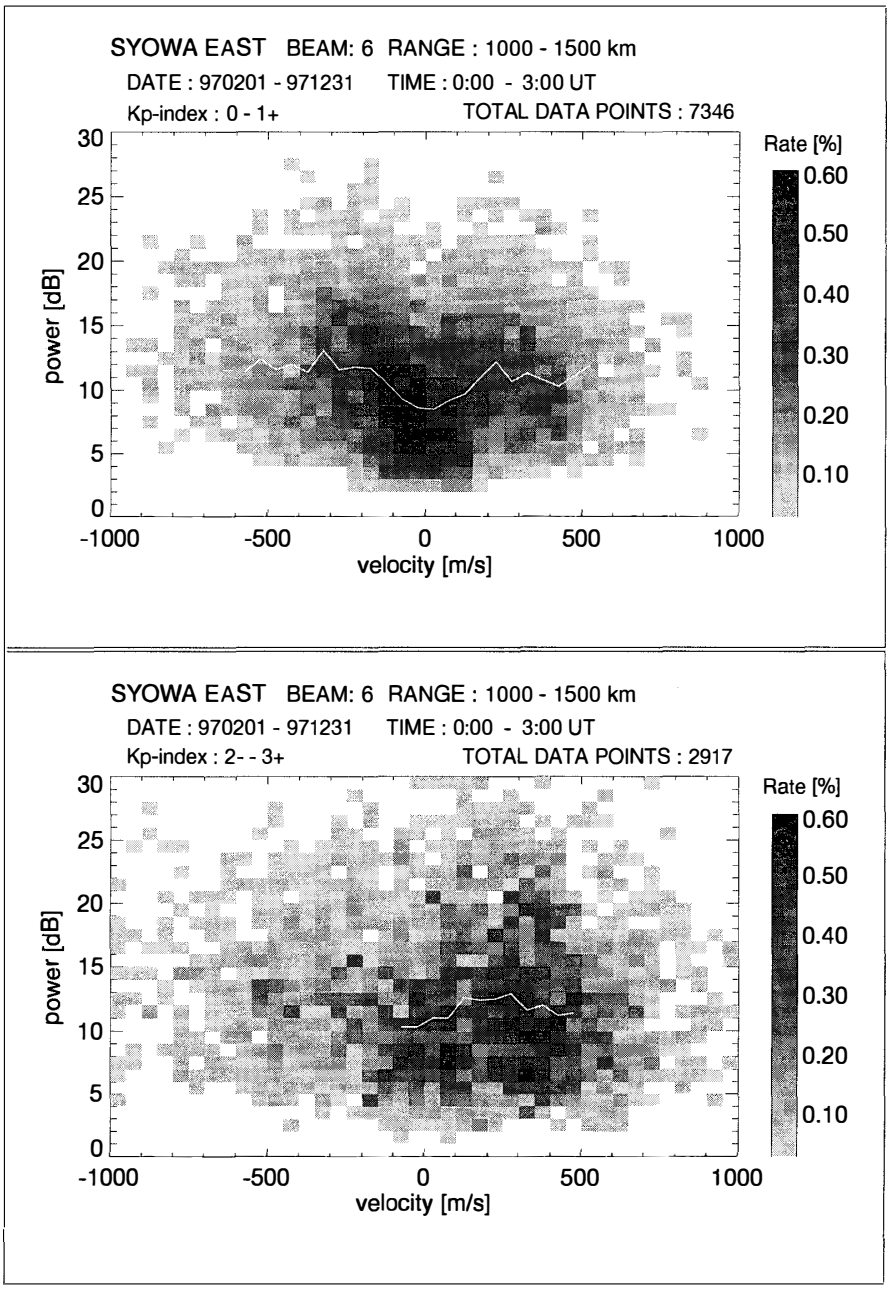

Fig. 4. K_p dependence of the relationship between echo power and Doppler velocity for the time interval of 0–3 UT (1–4 MLT). The upper panel shows the data obtained under quiet conditions ($K_p = 0$ to 1+), while the lower panel shows the data obtained under disturbed conditions (K_p = 2– to 3+).

F region irregularities is affected by other mechanisms related to particle precipitation, such as current-convective instability. As a result, the correlation between the echo power and Doppler velocity is weakened. In other time sectors, such as 21–24 UT (22–01 MLT), the dependence on the K_p index is not observed. Figure 5 shows the relationship between the echo power/Doppler velocity correlation and the K_p index for the time interval of 21–24 UT (22–01 MLT). In this time sector, a positive correlation is not present, even under quiet conditions (upper panel). This result suggests that the effect of particle precipitation on the generation of F region irregularities may be dominant even

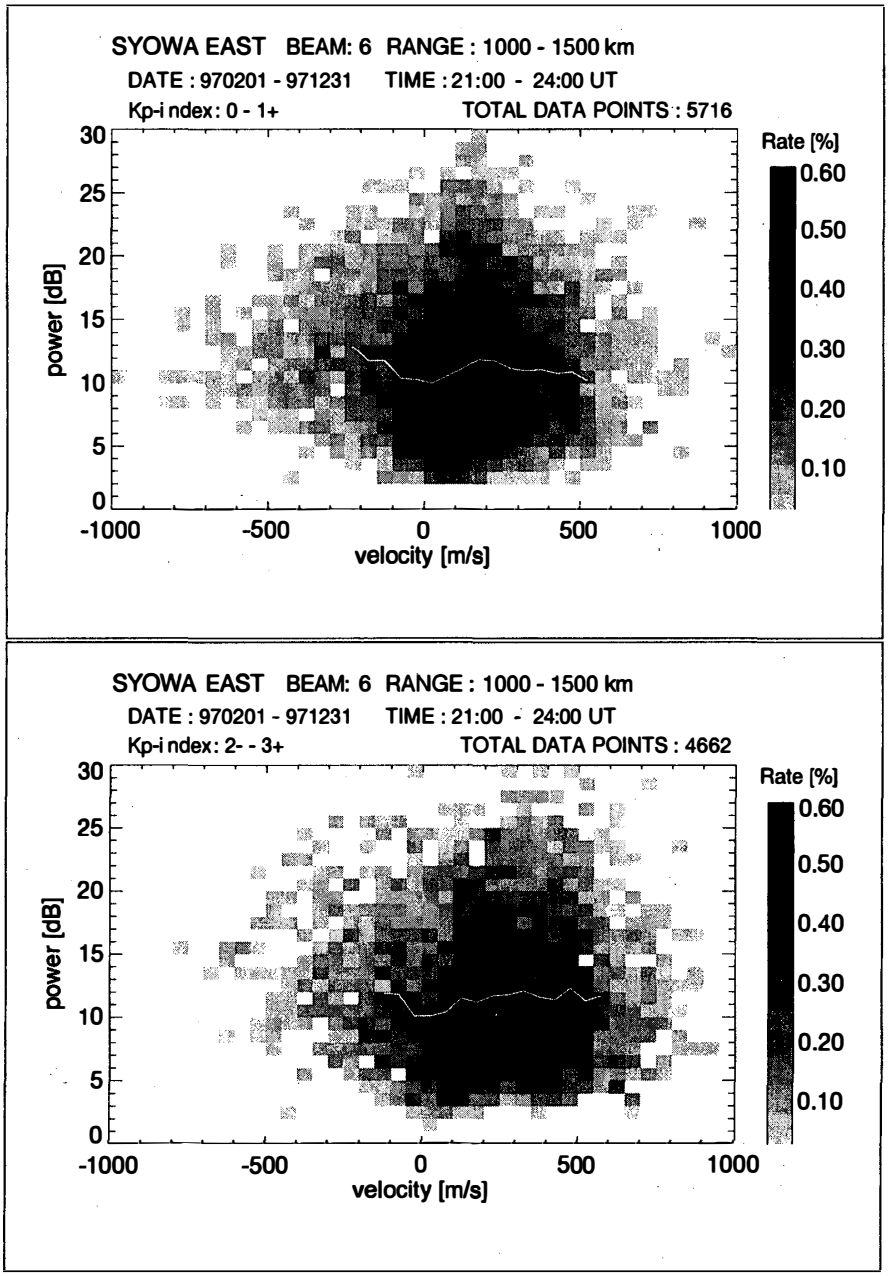

Fig. 5. K_p dependence of the relationship between echo power and Doppler velocity for the time interval of 21–24 UT (22–01 MLT). The upper panel shows the data obtained under quiet conditions ($K_p = 0$ to $1+$), while the lower panel shows the data obtained under disturbed conditions ($K_p = 2-$ to $3+$).

under quiet conditions, resulting in a poor correlation.

3. Discussion and conclusion

To clarify the mechanisms by which decameter-scale irregularities are generated, we investigated the relationship between the echo power and the Doppler velocity of HF radar echoes from the high-latitude *F* region ionosphere. Several instabilities have been proposed to account for these high-latitude ionospheric irregularities. Tsunoda (1988) stated that gradient-drift and current-convective instabilities are the main mechanisms responsible for generating these irregularities. Gradient-drift instability is characterized by a density gradient that is aligned with the $\boldsymbol{E}\times\boldsymbol{B}$ drift direction. In current-convective instability, the field-aligned currents and the parallel component of the irregularities' wave length ($k_{\parallel}$) play important roles in the creation of a polarized electric field that unstabilizes the system. Since nonlinear theories are not available for comparing these instabilities with our observational results, we discuss our results on the basis of linear theories.

According to linear theory, the growth rate of the gradient-drift instability (γ_1) is proportional to the ambient electric field such that $\gamma_1 \propto E_0/L$ (Ossakow and Chaturvedi, 1979), where E_0 and L are the ambient electric field and the density gradient scale length, respectively. If E_0 becomes stronger, the growth rate increases and the irregular amplitude of the plasma density grows faster and reaches a higher level. On the other hand, the growth rate of the current-convective instability (γ_2) is proportional to the field-aligned current velocity such that $\gamma_2 \propto V_d/L$ (Ossakow and Chaturvedi, 1979), where V_d is the field-aligned drift velocity of the electrons relative to the ions. Thus, the growth rate of this instability is independent of the electric field. The echo power of HF radar depends on the crosssection of the irregularity, or the mean of the density fluctuations (Hanuise *et al.*, 1991).

Since the Doppler velocity of the backscattered echo corresponds to the $\boldsymbol{E}\times\boldsymbol{B}$ plasma drift, the Doppler velocity is proportional to the electric field. Therefore, the mean of the density fluctuations that are associated with gradient-drift instability is also proportional to the Doppler velocity. As a result, the echo power from the irregularities should increase when the Doppler velocity increases if the irregularities are produced by gradient-drift instability. In contrast, if the irregularities are associated with current-convective instability, the echo power should not increase when the Doppler velocity increases because the linear growth rate of the current-convective instability is independent of the electric field.

In general, a positive correlation is seen between the echo power and the Doppler velocity, as shown in Fig. 2. This correlation suggests that the irregularities are mainly associated with gradient-drift instability, as discussed above. However, the relationship is poor around the afternoon and midnight sectors, as shown in Fig. 3. We speculate that in these time sectors, the generation of the irregularities is affected by other mechanisms that are related to particle precipitation (field-aligned current), such as current-convective instability. The effect of particle precipitation on the relationship between echo power and Doppler velocity is indicated in Fig. 4. The clear positive correlation in the upper panel (quiet conditions) becomes unclear in the lower panel (disturbed conditions). Since

precipitation increases with increasing geomagnetic activity (*e.g.*, Hardy *et al.*, 1985), the result shown in Fig. 4 suggests that an increase in particle precipitation is the cause of poor correlation. Therefore, we believe that the poor correlations around the afternoon and midnight sectors are due to the effect of the field-aligned currents on the mechanism of irregularity generation.

The statistical distribution of large-scale field-aligned currents reported by Iijima and Potemra (1976) is not consistent with the results of our analysis. The echo region used in this study is located around a magnetic latitude of 75°, while the high-latitude boundary of the large-scale field-aligned currents is located around 71° in the midnight sector. However, spatially localized, smaller scale field-aligned currents are observed elsewhere in the polar region, and this type of field-aligned currents may play an important role in the generation of irregularities.

Velocity shear driven instability is another possible mechanism that may be involved in the generation of irregularities (*e.g.*, Basu *et al.*, 1988, 1990). Since intense velocity shear regions and strong field-aligned current regions occupy the same spatial positions, the relative importance of velocity shear instability to other instabilities, such as current-convective instability, is difficult to estimate. Nevertheless, the possible involvement of this kind of instability in the generation of *F* region irregularities should be considered.

Investigating the relationship among the parameters of backscattered echoes is a useful approach for clarifying the mechanisms by which ionospheric irregularities are generated. Unfortunately, no nonlinear theories for *F* region plasma instabilities presently exist. Nevertheless, we speculate that 1) for most of the local time sectors, the generation of *F* region irregularities is associated with gradient-drift instability, resulting in a positive correlation between the echo power and the Doppler velocity, and 2) the poor correlation between these parameters in some regions is due to the effect of other mechanisms related to the field-aligned current (particle precipitation), such as current-convective instability.

Acknowledgments

We would like to thank all the staff who contributed to the HF radar experiment at Syowa Station, Antarctica. The authors thank anonymous referees for their kind comments in reviewing the paper.

The editor thanks Dr. Jøran Moen and another referee for their help in evaluating this paper.

References

Baker, K.B. and Wing, S. (1989): A new magnetic coordinate system for conjugate studies at high latitude. J. Geophys. Res., **94**, 9139–9144.

Basu, Su., Basu, S., MacKenzie, E., Fougere, P.F., Coley, W.R., Maynard, N.C., Winningham, J.D., Sugiura, M., Hanson, W.B. and Hoegy, W.R. (1988): Simultaneous density and electric field fluctuation spectra associated with velocity shears in the auroral oval. J. Geophys. Res., **93**, 115–136.

Basu, Su., Basu, S., MacKenzie, E., Coley, W.R., Sharber, J.R. and Hoegy, W.R. (1988): Plasma structuring by the gradient drift instability at high latitudes and comparison with velocity shear

driven processes. J. Geophys. Res., **95**, 7799–7818.
Fukumoto, M., Nishitani, N., Ogawa, T., Sato, N., Yamagishi, H. and Yukimatu, A.S. (1999): Statistical analysis of echo power, Doppler velocity and spectral width obtained with the Syowa South HF radar. Adv. Polar Upper Atmos. Res., **13**, 37–47.
Greenwald, R.A., Baker, K.B., Hutchins, R.A. and Hanuise, C. (1985): An HF phased-array radar for studying small-scale structure in the high-latitude ionosphere. Radio Sci., **20**, 63–79.
Hanuise, C., Villain, J.P., Cerisier, J.C., Senior, C., Ruohoniemi, J.M., Greenwald, R.A. and Baker, K.B. (1991): Statistical study of high-latitude E-region Doppler spectra obtained with SHERPA HF radar. Ann. Geophys., **9**, 273–285.
Hardy, D.A., Gussenhoven, M.S. and Holeman, E. (1985): A statistical model of auroral electron precipitation. J. Geophys. Res., **90**, 4229–4248.
Iijima, T. and Potemra, T.A. (1976): The amplitude distribution of field-aligned currents at northern high latitude observed by Triad. J. Geophys. Res., **81**, 2165–2174.
Keskinen, M.J. and Ossakow, S.L. (1983): Theories of high-latitude ionospheric irregularities: A review. Radio Sci., **18**, 1077–1091.
Ogawa, T. and Igarashi, K. (1982): VHF radar observation of auroral E-region irregularities associated with moving-arcs. Mem. Natl Inst. Polar Res., Spec. Issue, **22**, 125–139.
Ogawa, T., Hirasawa, T., Ejiri, M., Sato, N., Yamagishi, H., Fujii, R. and Igarashi, K. (1990): HF radar experiment at Syowa Station for the study of high-latitude ionosphere-2: A capability (extended abstract). Proc. NIPR Symp. Upper Atmos. Phys., **3**, 91–95.
Ossakow, S.L. and Chaturvedi, P.K. (1979): Current convective instability in the diffuse aurora. Geophys. Res. Lett., **6**, 332–334.
Ruohoniemi, J.M. and Greenwald, R.A. (1996): Statistical patterns of high-latitude convection obtained from Goose Bay HF radar observations. J. Geophys. Res., **101**, 21743–21763.
Ruohoniemi, J.M. and Greenwald, R.A. (1997): Rates of scattering occurrence in routine HF radar observations during solar cycle maximum. Radio Sci., **32**, 1051–1070.
Tsunoda, R.T. (1988): High-latitude *F*-region irregularities: A review and synthesis. Rev. Geophys., **26**, 719–760.

(Received December 2, 1999; Revised manuscript accepted March 31, 2000)